

# CHARACTERIZATION OF THE RF FINGERS CONTACT FORCE FOR THE LHC WARM VACUUM BELLOW MODULES

C. Blanch Gutiérrez, V. Baglin, G. Bregliozzi, R. Kersevan, P. Chiggiato  
CERN, Geneva, Switzerland

## Abstract

Along the 27 Km of LHC beam pipe, various types of vacuum bellow modules are needed to compensate the mechanical misalignments of the vacuum chambers during installation and to absorb their thermal expansion during the bake-out. In order to reduce the beam impedance during operation with beams these modules are equipped with RF bridges to carry the image current. They are usually made out of a copper tube insert at one side and Cu-Be RF fingers at the other end of the module. A spring is used to keep the contact between the RF fingers and the tube insert. The geometry and the choice of this spring become critical to ensure a good electrical contact.

In this paper, a description of the test bench used to measure the contact force together with the procedure applied and the measurements performed are given. A summary of the maximum radial and axial offsets between the RF fingers and the insert tube while keeping a good electrical contact is presented.

## INTRODUCTION

In the LHC vacuum system almost 200 different types of warm vacuum modules are installed, making a total number of more than 1800 units. With different length, diameter and/or inner aperture, each type of module, by means of the RF transition inside, must ensure a good electrical continuity between the adjacent chambers. This electrical continuity is provided by the RF fingers and the tube insert which make a proper path, without geometrical discontinuities, for the image current when the beam is circulating through, avoiding large local impedances and electrical breakdown [1].

The electrical contact between the RF fingers and the tube insert depends on the geometry of both parts as well as on a spring, which assures the force to keep the contact [2] [3].

In order to qualify this electrical contact a test bench was implemented to measure the contact force between the RF fingers and the tube insert. Two different non-standard RF inserts types, one circular and one hippodrome geometry have been firstly tested and a bunch of tests are foreseen to characterize the rest of RF inserts installed currently in the LHC vacuum system.

## THE TEST BENCH DESCRIPTION

### Mechanical Set Up

The test bench used (Fig. 1) is made with three manual translational stages which allow the movement in the

three axes. In one side of the test bench the RF fingers are fixed while in the other side the tube insert is attached.

With this set up, three degrees of freedom are allowed between both components of the RF bridge, being possible to set offsets positions in the three axes within a  $\pm 0.5$  mm precision.

The transition tube is wrapped with Kapton tape in order to insulate its electrical contact with all the RF fingers except one of them in which the contact force will be measured.

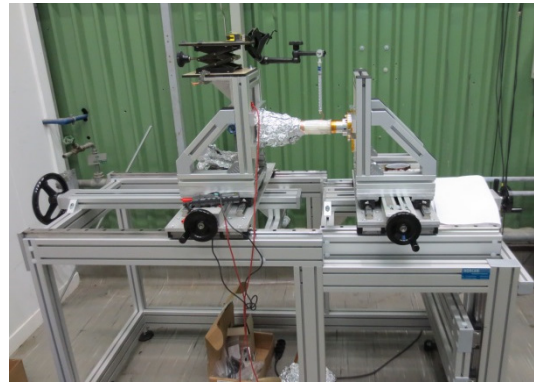


Figure 1: Test bench.

Above this finger a dynamometer attached to a mobile platform is placed. This dynamometer can measure in a range from 0 to 50g with a precision of 0.5g.

### Electrical Set Up

The electrical set up consists in a Keithley multimeter connected in 4-wires measurement resistance mode (Fig. 2), to measure the contact resistance between the RF finger and the transition tube.

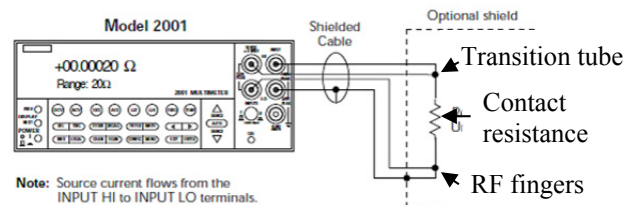


Figure 2: Electrical connection.

A different electrical set up was tested, applying 1 A constant current from the transition tube to the RF fingers, and measuring the voltage drop between them. Since  $R=\Delta V/I$  and  $I=1$  A, the voltage drop measured was equal to the resistance. However, since no difference or resolution improvement was observed with this second method, the first method was chosen for all the tests.

## TEST PROCEDURE

The method to measure the contact force follows the procedure here below:

1. The test bench was set in the nominal position, the spring was in place and the dynamometer attached to the top finger (the only one with electrical contact with the transition tube).
2. A low electrical resistance ( $\sim 3 \text{ m}\Omega$ ) [3] was measured, meaning a good contact.
3. The RF finger is pulled up by the dynamometer until the resistance increase considerably or open the circuit.
4. Read out the dynamometer, that indicates the force needed to open the contact: the contact force.

This procedure was repeated for different offsets in both axial and radial direction in steps of 5 mm for the axial offset and 1 mm for the radial offset.

## DEVICES TESTED

Two different non-standard RF inserts were tested, one circular geometry and one hippodrome geometry. Figure 3 and 4 show the drawings of both RF inserts.

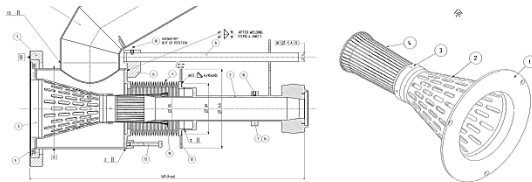


Figure 3: Circular insert.

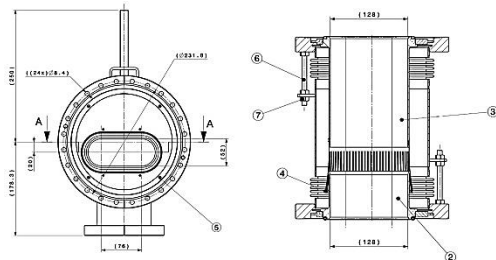


Figure 4: Hippodrome insert.

For the circular RF insert, since the spring applies the same force to every finger, the contact force must be the same, therefore only one finger position was measured. For the hippodrome RF insert, two fingers, one on the top flat zone and one in the middle of the circular part were tested since the spring does not apply the same force at the flat zone and at the round part.

## TEST RESULTS

### Circular RF Bridge

For the circular RF bridge, three different springs length were tested, 140, 149 and 160 mm, in order to choose the proper one and to study the behaviour of the contact force depending on the spring used [4]. The diameter and material were equal for all springs.

The axial offset was performed by moving the axial translation stage from the nominal position to  $\pm 20 \text{ mm}$  in steps of 5mm.

The radial offset was performed by moving the vertical translation stage from nominal position to  $-4 \text{ mm}$  and until the contact is completely lost in steps of 1 mm.

With the data obtained a contact force map was made. It includes the contact force measured for each of the three springs tested and for every offset position (Fig. 5).

Contact force (g)		AXIAL DISPLACEMENT (mm)																										
		-20			-15			-10			-5			0			5			10			15			20		
RADIAL DISPLACEMENT (mm)	Spring (mm)	140	149	160	140	149	160	140	149	160	140	149	160	140	149	160	140	149	160	140	149	160	140	149	160	140	149	160
	4	60	60	60	60	60	60	60	60	60	60	60	60	60	60	60	60	60	60	60	60	60	60	60	60	60	60	60
	3	60	60	60	60	60	60	60	60	60	60	60	60	60	60	60	60	60	60	60	60	60	60	60	60	60	60	60
	2	60	60	60	60	60	60	60	60	60	60	60	60	60	60	60	60	60	60	60	60	60	60	60	60	60	60	60
	1	30	60	45	29	44	35	28	39	30	35	40	28	40	43	30	60	40	32	43	60	40	47	60	60	60	60	60
	0	13	32	26	13	29	23	12	27	20	21	29	20	24	33	21	48	39	24	32	48	31	0	53	47	60	60	60
	-1	0	5	0	0	7	7	5	14	10	16	18	12	15	20	14	37	28	16	34	37	21	16	42	36	60	54	35
	-2	0	0	0	0	0	0	0	2	3	9	7	9	13	10	27	20	10	24	30	17	7	34	24	60	47	28	
	-3	0	0	0	0	0	0	0	0	0	0	0	0	4	2	17	13	7	11	22	12	0	28	19	46	42	23	
	-4	0	0	0	0	0	0	0	0	0	0	0	0	0	0	7	5	0	0	13	7	0	3	12	40	33	19	
-5	0	0	0	0	0	0	0	0	0	0	0	0	0	0	0	0	0	0	0	0	0	0	0	0	6	33	27	12
-6	0	0	0	0	0	0	0	0	0	0	0	0	0	0	0	0	0	0	0	0	0	0	0	0	0	26	18	4
-7	0	0	0	0	0	0	0	0	0	0	0	0	0	0	0	0	0	0	0	0	0	0	0	0	0	21	13	0
-8	0	0	0	0	0	0	0	0	0	0	0	0	0	0	0	0	0	0	0	0	0	0	0	0	0	5	0	0

Figure 5: Contact force map.

Figure 6 shows the contact force for every spring at nominal axial position for different radial offsets.

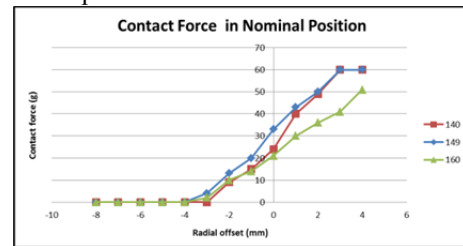


Figure 6: Contact force in nominal position.

In Fig. 6, it can be observed that the 149 mm long spring produces the largest contact force; it is even larger than using the 140 mm spring, which is shorter and therefore more stressed at the installation length, applying a larger force at the installation position but not increasing the contact force. This is due to the geometry of the RF fingers (bent at the end) which produces a lever effect lifting the RF finger at the contact point (Fig. 7).

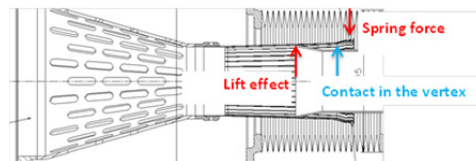


Figure 7: Lever effect.

The maximum radial offset at nominal axial position using the 149 mm spring is  $\pm 3 \text{ mm}$ . This range increases as the axial position as showed in Figure 8.

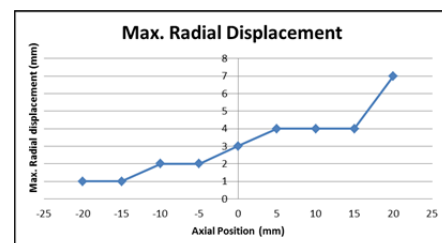


Figure 8: Maximum radial offset at which the electrical contact is preserved, as a function of the axial position.

### Hippodrome RF Bridge

For the hippodrome RF bridge, the axial offset range measured was  $\pm 10$  mm from nominal position, in steps of 5 mm. Whereas the radial offset range measured was  $\pm 3$  mm from nominal position in steps of 1 mm.

The contact force map for both measured fingers is shown in the figures below.

Contact force (g)	Axial offset (mm)				
	-10	-5	0	5	10
3	0	0	0	0	0
2	9	2	0	0	0
1	31	16	9	4.5	2
0	46	29	20	10	6.5
-1	60	40	30	17	11
-2	60	60	38	22	16
-3	60	60	48	30	22

\* Contact force = 60g means out of range, >50g

Figure 9: Contact force map (left - finger on flat zone, right - finger on circular zone).

The map shows that at nominal axial position, the maximum radial offset is 1 mm before the RF finger start losing the contact.

The same data is represented in the contour plot below (Fig. 10), representing the range of contact force in radial against axial offset graphic.

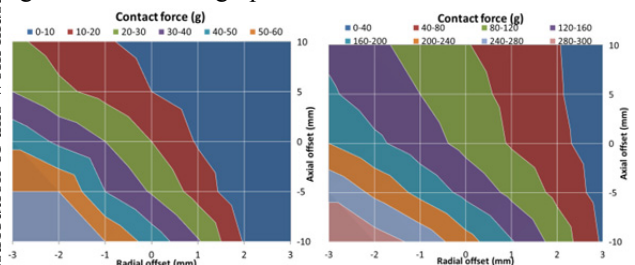


Figure 10: Contour plot (left - finger on flat zone, right - finger on circular zone).

### F.E.A. Comparison

The hippodrome insert was modelled in Ansys in order to evaluate the contact force on the fingers by Finite Elements Analysis and compare the results with the empirical test. To simplify the model and to reduce the computing time, only a quarter was analysed applying symmetry boundary conditions. The model was meshed with shell elements.

Large displacements analysis with two load steps was performed. The first step slides the RF fingers on the tube insert up to the nominal position; the second step applies the load produced by the spring to the RF fingers. Figure 11 shows the Von-Mises stress at nominal position.

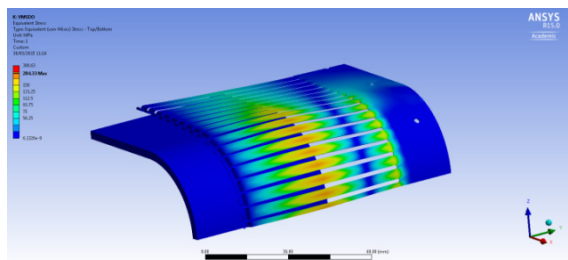


Figure 11: Von-Mises stress.

The contact force obtained for the nominal position was 0.22 N for the top finger on the flat zone and 0.98 N for the finger on circular zone. Similar results were obtained

in the test bench, i.e. 20 g ( $\approx 0.20$  N) and 108 g ( $\approx 1.06$  N) respectively; as a consequence the model is validated (Fig. 12).

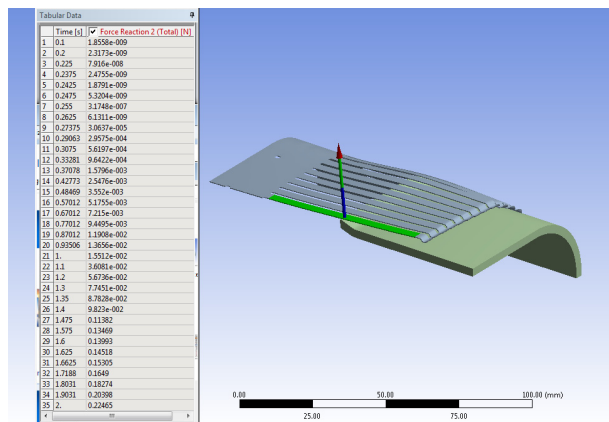


Figure 12: Model for the calculation of the contact force.

## CONCLUSIONS

The test bench showed to be a good way both to characterize the RF bridges behaviour in terms of electrical contact and to choose the proper spring, performing a good repeatability and accuracy.

The working range (range of radial offsets in which the electrical contact is ensured) in nominal axial position of the non-standard circular RF bridge tested ( $\pm 3$  mm) looks good enough for absorbing any mechanical misalignments of the vacuum module. However, in the case of the hippodrome RF bridge, this range is more narrow ( $\pm 1$  mm); therefore, a more careful installation and alignment would be required for this module.

The FEM analysis showed good correlations with the experimental data. Such results prove the usefulness of FEM analysis for future designs.

## FORESEEN WORK

A bunch of test is planned in the next months following the same procedure in order to characterize the rest of RF bridges installed in the LHC beam pipes.

In addition, a new contact force measurement method based on thin piezoelectric film sensor will be used to achieve more accurate and faster tests.

Although there are some contact force specifications in [3], an impedance test should be done in order to clearly define the minimum contact force admissible.

## REFERENCES

- [1] LHC Design Report.
- [2] E. Metral et al., "Lessons learnt and mitigation measures for the CERN LHC equipment with RF fingers", TUPWA042, IPAC'13, Shanghai, China.
- [3] R. Veness et al., "Design aspects of the RF contacts for the LHC beam vacuum interconnectors", PAC'01, Chicago, USA.
- [4] C. Blanch, CERN, EDMS 1391490.

Any distribution of this work must maintain attribution to the author(s), title of the work, publisher, and DOI.